EFFICIENT ORBIT INTEGRATION BY ORBITAL LONGITUDE METHODS

Toshio FUKUSHIMA
National Astronomical Observatory of Japan
2-21-1, Ohsawa, Mitaka, Tokyo 181-8588, Japan
E-mail: Toshio.Fukushima@nao.ac.jp

Abstract

Recently we developed a new formulation of numerical integration of orbital motion named *manifold correction methods* [4, 5, 6, 7, 8, 9]. The main trick is to keep rigorously the consistency of some physical relations such as that of the orbital energy, of the orbital angular momentum, or of the Laplace integral of a binary subsystem. This maintenance is done by applying a sort of correction to the integrated variables at every integration step. Typical methods of correction are certain geometric transformation such as the spatial scaling and the spatial rotation, which are commonly used in the comparison of reference frames, or mathematically-reasonable operations such as the modularization of angle variables into the standard domain $[-\pi, \pi)$. The finally-evolved form of the manifold correction methods is the orbital longitude methods [9, 10, 11, 14], which enable us to conduct an extremely precise integration of orbital motions. In the unperturbed orbits, the integration errors are suppressed at the machine epsilon level for an infinitely long period. In the perturbed cases, on the other hand, the errors initially grow in proportion to the square root of time and then increase more rapidly, the onset time of which depends on the type and the magnitude of perturbations. This feature is also realized for highly eccentric orbits by applying the same idea to the KS-regularization [12, 13, 15]. Especially the introduction of time element greatly enhances the performance of numerical integration of KS-regularized orbits whether the scaling is applied or not.

1 METHODS OF MANIFOLD CORRECTION

In short, the new method is a modern revival of Nacozy's original idea [19] to correct the integrated orbits during the integration process to ensure that they exactly lie on a certain manifold containing the true solution such as an energy-constant hypersurface by a kind of projection operation. It was first named as the methods of *manifold correction* by Murrison [18]. Later Hairer discussed it independently and called it the *projection method* [16].

The simplest example [4] of the manifold correction is to maintain the Kepler energy relation,

$$K = T - U \tag{1}$$

where $T \equiv \vec{v}^2/2$ is the kinetic energy and $U \equiv \mu/r$ is the (negative) gravitational potential energy. The correction is achieved to all the binary subsystems by applying the single spatial scaling,

$$(\vec{x}, \vec{v}) \to (\sigma\vec{x}, \sigma\vec{v}), \tag{2}$$

at every integration step. This form of correction was motivated by a theoretical examination of the manner of error growth of a circular motion by the simplest integrator, the Euler method [4]. Here the scale factor σ is determined from the solution of an associated cubic equation,

$$T\sigma^3 - K\sigma - U = 0, \tag{3}$$

numerically by means of the Newton method starting from an obvious initial guess $\sigma_0 = 1$.

See Figure 1, which compares the error growth of a Keplerian orbit obtained by the standard method to integrate the equation of motion in rectangular coordinates directly and that with

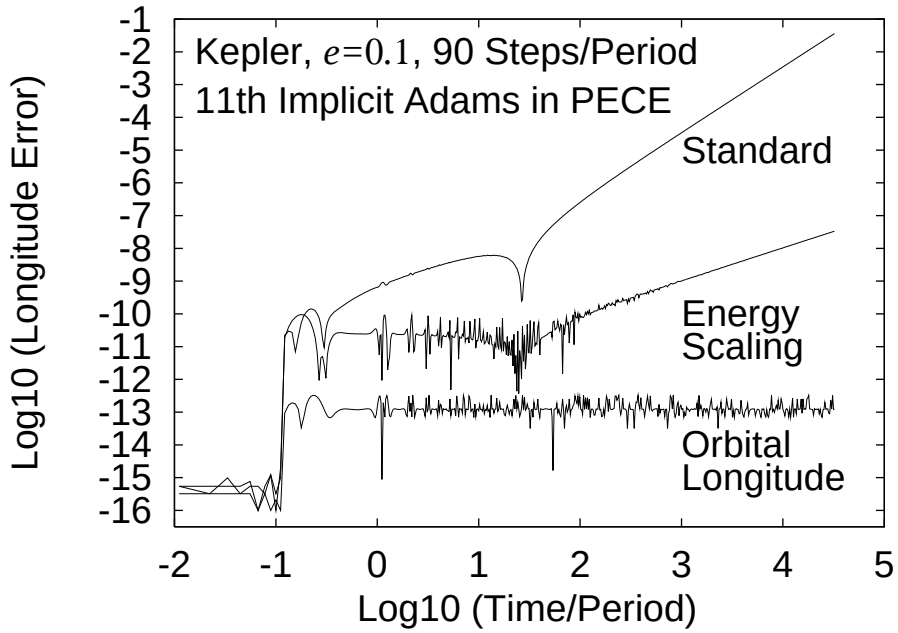

Figure 1: Illustrated are the errors in the mean longitude at epoch as functions of time in a log-log scale. Integrated was a moderately eccentric ($e = 0.1$) Keplerian orbit by (1) the standard method to integrate directly in rectangular coordinates, (2) the scaling method for Kepler energy consistency [4], and (3) the antifocal longitude method [11]. The adopted integrator was the eleventh order implicit Adams method in the PECE mode (predict, evaluate, correct, evaluate), the step size was fixed through the integration and set as 1/90 the orbital period, the starting tables were prepared by Gragg's extrapolation method, and the errors were measured by comparing with the reference solutions obtained by the same method, the same integrator, and the same model parameters but with half the step size. Since the order of the integrators are sufficiently high, halving the step size eliminates almost all the truncation errors.

the aforementioned single scaling for the Kepler energy, K, which becomes a constant in this unperturbed case. This figure shows that the well-known quadratic increase of the integration errors is reduced to a linear growth, which has been observed for a limited type of integration scheme; the symplectic integrator and the symmetric linear multistep method. The observed difference in the rate of error growth, which was partially enhanced by the introduction of some Encke-like technique to reduce the effect of round-off error accumulation [3], will lead to a large difference in the magnitude of integration error in the long run.

In case of perturbed orbits, the Kepler energy is no more a constant. Then we follow its time development by integrating its equation of motion simultaneously with that of the position and velocity. The good performance of the scaling method is unchanged as seen in Figure 2, which illustrates an example of n-body integration; Mercury's error growth in the integration of the Sun and nine major planets.

The effectiveness of manifold correction methods is independent on various aspects of the orbit integration such as the method of integration (Runge-Kutta, extrapolation, or linear multistep), the type of base orbits (elliptic, parabolic, or hyperbolic), the kind of perturbations (autonomous or not, conservative or not, velocity-dependent or not, etc.) [4].

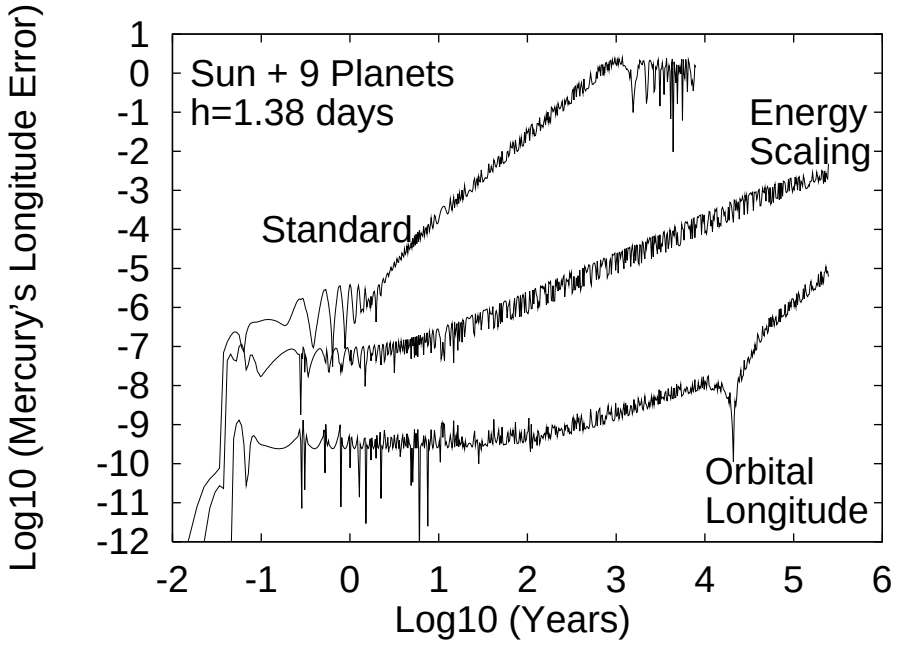

Figure 2: Same as Figure 1 but for the longitude error of Mercury in the simultaneous integration of the Sun and nine major planets for half a million years. The step size was chosen relatively large as around 1.4 days.

2 ORBTIAL LONGITUDE METHODS

The Kepler energy is not the only quantity suitable to be monitored for the manifold correction. Any quasi-conserved quantity can be used additionally. Then we refined the single scaling method by adding such quantities as (1) a quantity related to the Laplace integral [5], (2) the orbital angular momentum [6], and (3) the full Laplace integral vector [7]. Such extensions enhance the performance but at the cost of increase of computational effort.

Next we developed some simplified version of the last evolved form, the linear transformation method [7], by reducing the complexity of the manifold correction by some sets of variable transformation [8, 9]. Finally we arrived a method requiring *no* manifold correction, which we named the (original) orbital longitude method [9]. The method uses a set of six variables consisting of (1) $\vec{L}$ as the three rectangular components of the orbital angular momentum, (2) g as a true orbital longitude measured from a certain longitude origin solely determined from $\vec{L}$, and (3) P_A and P_B as the two on-the-plane components of the Laplace integral vector.

To our surprise, the application of the modularization of angle g into the standard range $[-\pi, \pi)$ at every integration step leads to *no* growth of integration error if the integration method is sufficiently precise, say the eleventh order implicit Adams method with the step size as 1/90 the orbital period [10]. The true longitude is not the only orbital longitude to be used. By replacing it with the antifocal longitude, we enhanced its performance further [11]. Here the antifocal longitude is an orbital longitude with the coordinate origin as not the primary focus but the secondary one.

See Figure 1 again which shows the superiority of this antifocal longitude method over the standard and the single scaling method. Note that this slowness of the error increase also means that the accumulation of round-off errors, which is usually expected to grow in the 1.5 power of the time, is also suppressed. As far as the author knows, this is the first exception of

Brouwer's law [2]. We think that this exceptional phenomenon was caused by transforming the second-order differential equation in rectangular coordinates to the first-order one in the orbital longitude. Its example is the equation of time development of true anomaly in the Keplerian motion,

$$\frac{\mathrm{d}f}{\mathrm{dt}} = \nu(1 + e\cos f)^2 \quad \text{where} \quad \nu \equiv n\left(1 - e^2\right)^{-3/2}, \tag{4}$$

which is nothing but a rewriting of Kepler's second law or the defining relation of the angular momentum.

In fact, we observed that the presence of the perturbations only enlarges this zero-growth to the square-root-growth as was already observed in Figure 2. This low rate of error growth is understood by the statistical accumulation of zero-mean random errors. Of course, this is only for some initial phases and the actual integration errors will increase more rapidly when the truncation errors become dominant. In any sense, these changes in the manner of error growth has led to a drastic decrease of the overall integration errors as seen in Figures 1 and 2.

Recently, we elaborated these orbital longitude methods by introducing Sundmann's time transformation [14], which enhances the original orbital longitude methods especially in the highly eccentric cases.

3 APPLICATION TO KS-REGULARIZED MOTION

The concept of the manifold correction is not limited to the direct integration in rectangular coordinates. Since the two orbital longitude methods [9, 10, 11] loose their efficiency in highly eccentric cases, we applied the same idea to the Kustaanheimo-Stiefel (KS) regularization.

In terms of the KS-regularized orbital motion, the Kepler energy relation reduced to that of, H, the total energy of the four-dimensional harmonic oscillator, $\vec{u}$, associated to the regularization;

$$H = T + V, \tag{5}$$

where $T \equiv (\vec{u}')^2/2$ and $V \equiv -(K/2)\vec{u}^2$ are the kinetic and potential energies of the associated four-dimensional harmonic oscillator, and $'$ denotes the differentiation with respect to the fictitious time, s, the independent variable in the KS regularization. Again the correction is done by the single scaling. This time the scale factor is explicitly evaluated as

$$\sigma = \sqrt{\frac{\mu}{4(T+V)}}. \tag{6}$$

In late 1970's, Mikkola invented a similar device to correct the KS variables to maintain the orbital energy (E) and the magnitude of the orbital angular momentum (J) of a binary subsystem. Then Aarseth named it the *EJ scaling* [1]. We confirmed that the single scaling to maintain the Kepler energy consistency in terms of the KS variables is slightly better than the EJ scaling [12]. Next we developed it into the quadruple scaling method, which adjusts all the four components of the harmonic oscillator associated with the KS regularization [13].

See Figure 3 showing the performance of these two scaling methods. Again the scaling reduces the error growth rate from quadratic to linear in the long run, although the appearance of some amount of periodic errors are unchanged. The quadruple scaling provides the better performance. However, we should note that this is at the cost of increase of variables to be integrated simultaneously from 10 to 13.

Unfortunately, even the quadruple scaling method could not achieve the zero growth of integration error. Therefore we examined the origin of the quadratic and linear error growth in the KS regularization with and without the scaling.

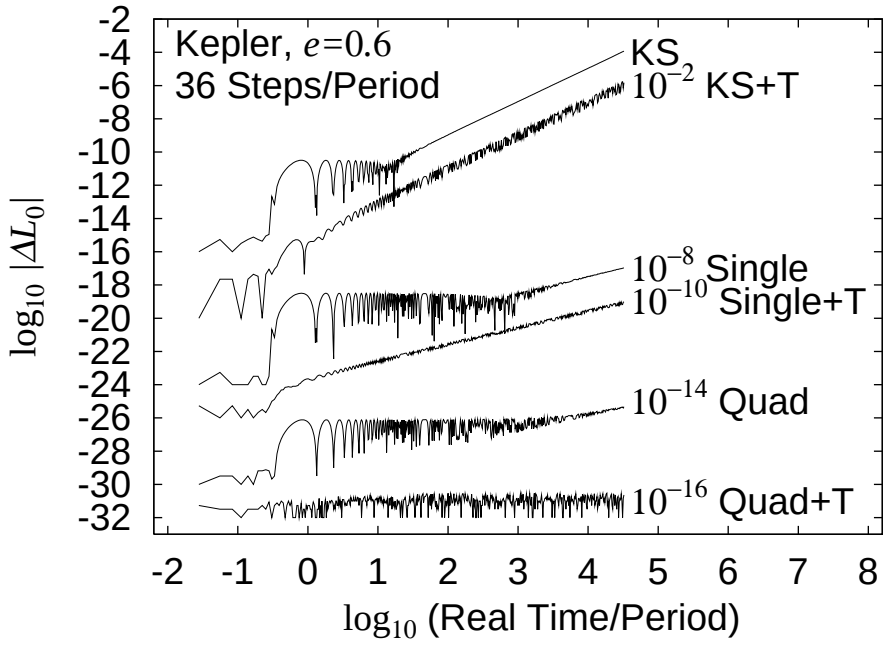

Figure 3: Similar as Figure 1 but for a highly eccentric ($e = 0.6$) orbit integrated by the methods using the KS regularization; (1) the original KS regularization [20], (2) the single scaling method [13], (3) the quadruple scaling method [13], (4) the KS regularization using the time element in a primitive form, (5) the single scaling using the time element [15], and (6) the quadruple scaling using time element [15]. The symbol '+T' denotes the usage of time element. Most of the curves are multiplied with some factors to avoid an overlap with others. The step size in the fictitious time was fixed through the integration and made so large that one orbital period in the real time is covered by only 36 steps. The order of the Adams method was set as that led to the least errors; the 13th for the two methods of quadruple scaling, and the eleventh for the others.

During the course of investigation, we unexpectedly discovered that the integration error of a harmonic oscillator can be reduced to achieve the zero-growth manner if the integrator adopted is sufficiently precise. Also we found that the cause of total error growth lies in integrating the development equation of physical time

$$t' = r \equiv \vec{u}^2. \tag{7}$$

Once Stiefel [20] proposed to integrate not the physical time, t, but its function named the *time element*, τ, defined as

$$\tau \equiv t - \left(\frac{1}{K}\right) \vec{u} \cdot (\vec{u})' . \tag{8}$$

A primitive form of the equation of motion of τ becomes as

$$\tau' = r - \left(\frac{1}{K}\right) \left[(\vec{u})'\right]^2 + \cdots , \tag{9}$$

where we omitted the terms reducing to zero in the case of unperturbed motion. Adoption of this primitive form leads to the supression of periodic part whose appearance is eminent in the initial phases as seen in Figure 3.

On the other hand, if one rewrites the first two terms by using the Kepler energy relation, the above equation of motion is further simplified as

$$\tau' = -\left(\frac{\mu}{2K}\right) + \cdots , \tag{10}$$

where the first term remains to be a constant in the limit of unperturbed case. Namely the motion of the time element reduces to a linear function of the fictitious time in the limit of unperturbed orbits, which can be integrated error-free by any kind of proper integrator. We confirmed that the combination of this elaborated form and the quadruple scaling guides us to the zero growth of unperturbed orbit integration in the KS-regularized formulation as was already shown in Figure 3.

In any case, the magnitude of the periodic error observed commonly in the KS regularization integrating the physical time, t, no longer appears after its replacement by the time element, τ.

References

[1] Aarseth, S.J., 2003, Gravitational N-body simulations, (New York: Cambridge Univ. Press)

[2] Brouwer, D., 1937, Astron. J., 46, 149

[3] Fukushima, T., 1996, Astron. J., 112, 1263

[4] Fukushima, T., 2003a, Astron. J., 126, 1097

[5] Fukushima, T., 2003b, Astron. J., 126, 2567

[6] Fukushima, T., 2003c, Astron. J., 126, 3138

[7] Fukushima, T., 2004a, Astron. J., 127, 3638

[8] Fukushima, T., 2004b, Astron. J., 128, 920

[9] Fukushima, T., 2004c, Astron. J., 128, 1446

[10] Fukushima, T., 2004d, submitted to Celest. Mech. Dyn. Astr.

[11] Fukushima, T., 2004e, Astron. J., 128, 1455

[12] Fukushima, T., 2004f, Astron. J., 128, No.6

[13] Fukushima, T., 2004g, Astron. J., 128, No.6

[14] Fukushima, T., 2005a, Astron. J., 129, No.2

[15] Fukushima, T., 2005b, Astron. J., 129, accepted

[16] Hairer, E., Lubich, C., and Wanner, G. 1999, Geometric Numerical Integration, Springer-Verlag, Berlin

[17] Kustaanheimo, P., and Stiefel, E.L., 1965, J. Reine Angew. Math. 218, 204

[18] Murison, M.A. 1989, Astron. J., 97, 1496

[19] Nacozy, P.E. 1971, Astrophys. and Space Sci., 14, 40

[20] Stiefel, E.L., and Scheifele, G., 1971, Linear and Regular Celestial Mechanics, (New York: Springer)